Global Precipitation Measurement (GPM): Unified Precipitation Estimation From Space

By: Gail Skofronick-Jackson, Wesley Berg, Chris Kidd, Dalia B. Kirschbaum, Walter A. Petersen, George J. Huffman, Yukari N. Takayabu

***Abstract*—Global Precipitation Measurement (GPM) is an international satellite mission that uses measurements from an advanced radar/radiometer system on a Core Observatory as reference standards to unify and advance precipitation estimates through a constellation of research and operational microwave sensors. GPM is a science mission focusing on a key component of the Earth's water and energy cycle, delivering near real-time observations of precipitation for monitoring severe weather events, freshwater resources, and other societal applications. This work presents the GPM mission design, together with descriptions of sensor characteristics, inter-satellite calibration, retrieval methodologies, ground validation activities, and societal applications.**

***Index Terms*—Precipitation retrievals, satellite, radiometers, radar.**

I. INTRODUCTION

The Global Precipitation Measurement (GPM) mission is an international satellite mission initiated by the National Aeronautic and Space Administration (NASA) and the Japan Aerospace and Exploration Agency (JAXA) to unify and advance global precipitation measurements from space (Hou et al., 2014). The mission centers on the deployment of a GPM Core Observatory (GPM-CO, launched February 2014) carrying a Ka/Ku-band Dual-frequency Precipitation Radar (DPR) and a multifrequency (10-183 GHz) microwave radiometer, the GPM Microwave Imager (GMI). The GPM-CO serves as a physics observatory of precipitating systems and a calibration reference for precipitation estimates from a constellation of microwave radiometers operated by a consortium of international partners (Hou et al., 2014). The mission

is designed to provide the next-generation, constellation-based global precipitation products for scientific research and societal applications (Skofronick-Jackson et al., 2017).

As a science-discovery mission with integrated applications goals, GPM's mission objectives are: (1) establishing new reference standards for precipitation measurements from space using combined active and passive remote-sensing techniques, (2) improving knowledge of precipitation systems, water cycle variability, and freshwater availability with enhanced measurements of the space-time distribution of global precipitation, (3) improving climate modeling and prediction capabilities through better measurements of latent heating, precipitation microphysics, and surface water fluxes, (4) improving weather forecasting skills with more accurate estimates of instantaneous precipitation information and error characterizations, and (5) improving hydrological modeling and prediction of high-impact natural hazard events (e.g., flood, drought, landslide, and hurricanes) through improved temporal sampling and high-resolution model-downscaled precipitation products. By making data available in near-real-time (NRT) to operational agencies and stakeholders beyond the traditional science community, GPM enables the use of space-based precipitation observations in a variety of practical applications to directly benefit society (Kirschbaum et al., 2017).

Building upon the success of the U.S.-Japan Tropical Rainfall Measuring Mission (TRMM) (Kummerow et al., 2000), GPM is a partnership between NASA and JAXA. NASA and JAXA provided the GPM-CO, which was launched on 28 February 2014 from Tanegashima Island in Japan. The GPM–CO has completed its prime mission life of 3 years and is now in extended operations. Remaining fuel projections are for operations to last into the 2030's if the batteries and instruments remain functional.

This chapter presents the GPM mission description in Section II, Core Observatory sensor capabilities in Section III, constellation coverage and sampling in Section IV, intercalibration of constellation radiometers in Section V, precipitation retrieval methodologies in Section VI, ground validation in Section VII, applications in Section VIII, and a summary in Section IX.

II. Mission Description

The GPM Core Observatory operates in a non-Sun-synchronous orbit at 65° inclination and an altitude of 407 km at the equator to permit diurnal observations of precipitation and coincident measurements with constellation radiometers to serve as a reference standard for the inter-calibration of both radiometric measurements and precipitation retrievals of the constellation members. The GPM-CO data are necessary for reducing the number of assumptions in the precipitation retrievals. This is because satellite rainfall estimates cannot be cast in terms of simple mathematical inversions. Precipitating clouds contain more free parameters (including their size, shape, and internal distribution of raining and non-raining water and ice particles) than can realistically be retrieved from a finite set of satellite measurements. Significant assumptions regarding the composition of clouds are therefore necessary (Stephens and Kummerow, 2007). GPM tackles this problem by first designing highly accurate instruments and second, by creating a common inventory of naturally occurring cloud states with details provided by the GPM-CO using the most advanced active and passive rainfall sensors. This inventory of clouds can then be used as the *a priori* state within a Bayesian or Optimal Estimation framework for constellation sensor retrievals (e.g., Kummerow et al., 2015). While the technique does not entirely eliminate the need for assumptions, it does employ the highly accurate GPM-CO data rather than less-capable radiometers or models to make the assumptions independently.

The 65° inclination for the GPM-CO was selected to offer broad latitudinal coverage without being locked into a Sun-synchronous low Earth orbit (LEO), while maintaining a relatively short precession period to sample the diurnal variability of precipitation. TRMM, at 35° inclination, has shown that the additional sampling afforded by asynoptic observations in between observations by LEO satellites at fixed local times are important for near real-time monitoring and prediction of hurricanes. The GPM-CO provides, for the first time, asynoptic observations for tracking mid-latitude and extratropical storms. The non-Sun-synchronous orbit also provides multiple coincident overpasses with the mostly LEO constellation sensors to facilitate inter-sensor calibration over a wide range of latitudes.

The GPM mission is supported on the ground by (1) a NASA-provided mission operations system for the

operation of the GPM Core, (2) a Ground Validation (GV) system consisting of dedicated and cooperative ground validation sites provided by NASA, JAXA, and an array of GPM ground validation partners, and (3) a NASA Precipitation Processing System (PPS) and a JAXA GPM Mission Operation System (GPM-MOS) in coordination with other GPM partner data processing sites to provide NRT and standard global precipitation products. For inter-satellite calibration, retrieval algorithm development, ground validation, and science applications, a NASA Precipitation Measurement Missions (PMM) Science Team and a JAXA PMM Science Team support GPM.

GPM is integral to international efforts to examine and understand the Earth's hydrological and energy cycles. The GPM mission is serving as the scientific cornerstone for a multi-national satellite constellation to monitor global precipitation under development by the Committee for Earth Observation Satellites (CEOS), and provides key measurements to advance the objectives of a host of international scientific programs and activities that include the Global Energy and Water Cycle Experiment (GEWEX), the Integrated Global Water Cycle Observations (IGWCO), and the International Precipitation Working Group (IPWG).

III. GPM Core Observatory Sensor Capabilities

TRMM focused primarily on moderate to heavy rain over tropical oceans. Since light rain (< 0.5 mm hr^{-1}) and falling snow account for significant fractions of the total precipitation events outside the tropics (Mugnai et al., 2007), improved measurements of these quantities are needed to gain a better understanding of global water fluxes and precipitation characteristics (e.g., frequency, intensity, distribution, etc.). The GPM-CO carries the first space-borne dual-frequency precipitation radar (DPR) at Ku and Ka bands capable of detailed microphysical measurements layer by layer within the cloud and a multi-spectral (10 to 183 GHz) GMI encompassing the range of frequencies typical of microwave imagers and humidity sounders. Specifications and on orbit performance is provided in Table 1. The active (DPR) and passive (GMI) sensors on board GPM-CO provide complementary information that are being used to improve the

fidelity of physically-based precipitation retrievals. The increased sensitivity of the DPR relative to the TRMM Precipitation Radar (PR) and the high-frequency GMI channels enable GPM to measure light rain (down to 0.2 mm hr^{-1}) and falling snow.

A. Dual-frequency Precipitation Radar (DPR)

The DPR instrument, which provides measurements of 3-dimensional precipitation structure, consists of a Ka-band Precipitation Radar (KaPR) at 35.5 GHz and a Ku-band Precipitation Radar (KuPR) at 13.6 GHz being an updated version of the Ku-band unit flown on TRMM (Kummerow et al., 1998). JAXA and the National Institute of Information and Communications Technology (NICT) of Japan built the DPR instrument. The KuPR and the KaPR are co-aligned such that their 5 km footprints coincide on the Earth surface, with cross-track swath widths of 245 km and 125 km, respectively (see Fig. 1), and a vertical range resolution of 250 m, except when the KaPR is operating in a high-sensitivity, spatial over-sampling mode, in which case the range resolution is 500 m. Both Ka and Ku oversample vertically to reduce the range distance by half. The variable pulse repetition frequency technique used by the DPR increases the number of samples at each Instantaneous Field-Of-View (IFOV) to achieve a detection threshold of 12 dBZ, or 0.2 mm hr^{-1}. The DPR has been calibrated both internally and externally through a series of Active Radar Calibration overpasses of calibrated ground sources provided by JAXA.

With information from the DPR, precipitation measurements are more accurate for retrieving two parameters of the bulk particle size distributions by using (1) the sensitivity of Ka to small particles, (2) the sensitivity of Ku to larger particles, and (3) a retrieval technique based on the differential attenuation between observations at the two frequencies. The dual-frequency returns give us insight into microphysical processes (evaporation, collision/coalescence, aggregation) and also allow us to distinguish regions of liquid, frozen and mixed-phase precipitation, in addition to providing bulk properties of the precipitation such as water flux (rain rate) and water content in the measurement column. The improved accuracy and detailed microphysical information from the dual-wavelength radar is used to constrain precipitation retrievals from the GMI and to develop an *a priori* Bayesian cloud model database to be used for

radiometer-based retrievals. This database is by the constellation radiometers to unify precipitation retrievals globally.

B. GPM Microwave Imager (GMI)

The GMI instrument is a multi-channel, conical-scanning, microwave radiometer characterized by thirteen channels ranging in frequency from 10 GHz to 183 GHz (Table 1), and a 1.2 m diameter antenna to provide better spatial resolution than TMI. The GMI has an off-nadir-viewing angle of 48.5 degrees, which corresponds to an earth-incidence-angle of 52.8 degrees, thus maintaining a similar geometry with the predecessor TRMM radiometer. The GMI main reflector rotates at 32 revolutions per minute to collect microwave radiometric brightness temperature (Tb) measurements over a 140 degree sector centered on the spacecraft ground track, giving a cross-track swath of 885 km on the Earth's surface from the GPM-CO 407 km altitude (see Fig. 1). The GMI was built by the Ball Aerospace and Technology Corporation under contract with NASA Goddard Space Flight Center. The central portion of the GMI swath overlaps the radar swaths with an approximately 67-second difference between the GMI and radar observation times (due to geometry and spacecraft motion). The measurements within the overlapped swaths of DPR and GMI are important for improving and cross-validating precipitation retrievals, especially the radiometer-based retrievals.

With the role of a reference radiometer in mind, the GMI is designed to achieve greater instrument accuracy and stability by employing several innovative engineering features. A high quality reflective coating was used on the main and cold calibration sub-reflectors. Noise diodes were included in the calibration scheme for the channels from 10.7 to 36.64 GHz enabling an explicit solution for non-linearity in the radiometer response functions (Draper et al., 2015a). The warm load has 14 temperature sensors imbedded in it to better characterize its physical temperature and any thermal gradients. The cold calibration sub-reflector is somewhat oversized to reduce spillover issues and the warm calibration load is shrouded to minimize solar intrusion. (Draper et al., 2013).

After launch, a series of spacecraft attitude maneuvers were performed to provide checks on and

refinements to the calibration. One of these maneuvers involved pitching up the GPM spacecraft so that both the main beam and the cold calibration mirror viewed cold space. The voltage from the radiometers was determined to be identical to within measurement uncertainty for both the main and sub-reflectors, indicating that either there are no significant emissivity issues for either reflector. A pitch down maneuver was also done to verify consistency between the vertical and horizontal polarizations at nadir for the dual-polarized channels and corrections were developed for calibration errors resulting from sensitivity of the radiometer to magnetic fields as well as updates to the pre-launch derived spillover corrections. This combination of the instrument design and detailed on-orbit calibration checks and refinements have resulted in an extremely stable and accurate calibration to within 0.5 K (Wentz and Draper, 2016).

IV. Coverage and Sampling

Given the current capabilities of microwave remote-sensing technology, the GPM mission takes a constellation-based approach by combining measurements from a constellation of microwave sensors in LEO to achieve global coverage and the high temporal sampling needed for a wide range of science and societal applications (Fig. 2). The GPM constellation was initially conceived to comprise conical-scanning radiometers, which have been the mainstay for rainfall estimation from space for many decades. Microwave sounding instruments, whose observations are less directly related to precipitation than conically scanning imagers, were not included in the original mission design. However, as retrieval algorithms for microwave sounders have continued to improve in recent years, the quality of current rainfall retrievals from microwave sounders with high-frequency channels between 150 and 183 GHz has been shown to be comparable to those from conical-scanning radiometers over land (Xin and Hou, 2008). The baseline GPM constellation was reconfigured in 2006 to include microwave sounding instruments to augment the sampling by conical-scanning radiometers over land, where revisit time is between 1 and 2 hours over the GPM mission life (Hou et al., 2014). The high-frequency sounding channels on GMI will also provide a bridge in using GPM-CO sensor measurements to further improve sounder retrievals in the GPM constellation.

The build-up of the GPM constellation follows a rolling wave strategy with a flexible architecture to take advantage of satellites of opportunity to provide the best possible sampling and coverage with assets provided by cooperating partners. The baseline constellation partner configuration in 2017 has 10 sensors including these conical-scanning imagers: the Advanced Microwave Scanning Radiometer -2 (AMSR-2) on Japan's Global Change Observation Mission-Water 1 (GCOM-W1) (Maeda et al., 2016), Special Sensor Microwave Imager/Sounder (SSMIS) instruments on three U.S. Defense Meteorological Satellite Program (DMSP) satellites (Kunkee et al., 2008). Cross-track scanning temperature/humidity sounders in the constellation in 2017 include: the Sondeur Atmosphérique du Profil d'Humidité Intertropicale par Radiométrie (SAPHIR) on the French-Indian Megha-Tropiques satellite (Roca et al., 2015), the Advanced Technology Microwave Sounder (ATMS) instrument on the National Polar-orbiting Operational Environmental Satellite System (NPOESS) Preparatory Project (NPP) (Goldberg et al., 2013), and four Microwave Humidity Sounder (MHS) instruments on NOAA and the European MetOp satellites (Klaese et al., 2007). Table 2 provides basic sensor and frequency details for the constellation sensors in the baseline configuration. Each constellation partner satellite radiometer has its own scientific or operational objectives but contributes microwave Tb observations to the GPM mission for unified constellation-based global precipitation products. The inter-satellite calibration (at both radiance and retrieval levels) using GPM-CO sensor measurements as reference standards within a consistent framework is a key objective of the GPM mission.

With such a constellation of varying precipitation sensors, inter-satellite calibration is an important aspect of the GPM mission. Indeed, GPM's multi-satellite Integrated Multi-satellitE Retrievals for GPM (IMERG; Huffman et al., 2017) provide precipitation estimates nearly globally every 30 minutes by using infrared (IR) observations to morph the precipitation estimates from the constellation sensors. The IMERG product is available at a surface resolution of 0.1° x 0.1° (or about 10 km x 10 km) in NRT about 5 hours after the precipitation event. All GPM-CO products are available in NRT for application users and also later as research products that include all ancillary data for better performance and lower uncertainty. The Japanese

counterpart of IMERG is the Global Satellite Mapping of Precipitation (GSMaP), provided also with 0.1° x 0.1°x 0.1° horizontal resolution and with various latencies; nowcast, 4 hours, etc. (Kubota et al., 2017). These products can be found at gpm.nasa.gov and at sharaku.eorc.jaxa.jp/GSMaP, respectively.

V. Radiance Intercalibration of Constellation Sensors

Climate quality data sets need to be accurate and consistent across long time periods spanning multiple observing platforms. Any Tb biases among the different GPM microwave constellation instruments might impede consistent global precipitation estimates. Despite similarities among these constellation sensors, differences exist in terms of center frequencies, viewing geometries, and spatial resolutions (Table 2), which must be reconciled in order to produce uniform global precipitation estimates. An important by-product of the cross calibration effort is the ability to monitor each instrument in the GPM constellation for abrupt and/or gradual calibration changes as well as other degradations.

Achieving consistency through intersatellite calibration requires several steps. First, each instrument provider is responsible for providing well-calibrated Tb products adhering to established standards. Based on these standard Tb products provided by partners, GPM examines the data to find and remove pixel-to-pixel biases that can be caused by pitch and roll errors, spacecraft interference and more subtle causes. For conical scanners, detecting biases is conceptually straightforward; the average Tb of each beam position should be the same. Biases due to latitude and small incidence angle anomalies are readily removed (Gopalan et al., 2009). For cross-track scanners detecting and correcting for biases to achieve self-consistency is much more difficult because the dependence on incidence angle must be very accurately modeled.

Once an instrument is shown to be self-consistent across a scan, it must be self-consistent through the orbit. For this purpose, environmental data such as Global Data Assimilation System (GDAS) is used to compute Tb for non-raining oceanic pixels throughout the orbit. While these calculations may not be adequate for absolute calibration, they are suitable for identifying Tb anomalies. When a consistent pattern of anomalies is detected, an approach is developed to correct for them.

Once individual instrument Tb are self-consistent, the multiple radiometers in the constellation are inter-calibrated to produce a uniform global Tb product within a consistent framework. To this end, GMI observations are spatially and temporally matched to the other constellation sensors. For the matched data sets, algorithm development precedes along two approaches (1) a system wherein co-located Tbs are translated to a common basis and compared (Hong et al., 2009; Berg et al., 2016), and (2) deriving limiting values for each radiometer independently and comparing them vicariously through a model (e.g., Brown and Ruf, 2005; Ruf et al., 2006). Corrections indicated by these matched comparisons are subsequently applied to constellation Tbs in the intercalibrated data files that are used as input for the radiometer retrieval algorithm (Berg et al., 2016).

VI. Precipitation Retrievals and Products

Unified precipitation estimation from a heterogeneous constellation of radiometric sensors requires not only robust intercalibration of Tb but also a physical framework for deriving rainfall with respect to a common standard. The GPM concept achieves this by using the GPM-CO to generate the best possible observed *a priori* statistics of precipitation profiles and their corresponding Tb at all channels observed by the diverse constellation radiometers. The GPM constellation radiometers then reference their own observations to this common *a priori* database to be physically consistent as envisioned in the mission concept. The GPM mission produces three types of precipitation products based on (1) DPR retrievals, (2) combined DPR/GMI retrievals, and (3) radiometer retrievals based upon *a priori* databases generated by the combined DPR/GMI retrievals. The DPR retrieval has been shown to provide the best retrieval when directly compared to surface radars (Kidd et al., 2017) and associated microphysical data that has historically been obtained from multi-parameter surface radars. The combined DPR/GMI retrieval is designed to begin with the DPR solution but modify this solution as necessary to ensure consistency not only with DPR reflectivities, but GMI radiances as well. This approach improves the overall results – particularly in scenes where the DPR is unable to fully describe the drop size distributions, the cloud liquid water content, or the rainfall falling below the detection threshold of the Ka band radar.

The radar algorithms take advantage of the sensitivity of the Ka and Ku bands to the underlying precipitation particles. The DPR's reflectivities provide two degrees of freedom at each range gate for determining the drop size distribution in the vertically sampled profile (Liao and Meneghini, 2005). This is a significant step forward, since TRMM and surface based radars rely on a single frequency and therefore require assumptions about the drop size distribution. The radar retrievals estimate profiles of the rain rate, liquid water content and parameters of the rain and snow particle size distributions as well as their associated error statistics. Special emphasis is focused on retrieval methods for very light rainfall cases, very heavy rainfall cases, and for falling snow cases (which were not retrieved with TRMM's orbit). With measurements at two frequencies, the DPR retrieval also benefits from the use of differential attenuation correction techniques instead of the more restrictive surface reference technique (Meneghini et al., 2000).

The combined radar-radiometer retrieval conceptually provides the best estimates of precipitation structure from a spaceborne platform through the combination of DPR and GMI information (Grecu et al., 2016). The retrieval naturally serves as the *a priori* cloud/precipitation database for precipitation retrievals from constellation radiometers. While this approach was used already with TRMM over tropical oceans, one of the challenges in GPM combined algorithm development was the creation of updated physical parameterizations for use at higher latitudes and for the enhanced channel sets of GMI and the DPR. Since freezing levels are lower at these latitudes, there is a need for the DPR to better identify the altitudes where the transitions from ice-phase to mixed-phase to liquid occur, in both convective and stratiform precipitation regions. In addition, improved descriptions of the extinction and scattering of ice and mixed-phase precipitation that are applicable to GMI's 10 – 183 GHz frequency range have been developed (e.g., Kuo et al., 2016; Olson et al., 2017). For GPM algorithm development improved physical parameterizations were supported by a series of ground validation field campaigns (see section VII).

The DPR, GMI, and Combined algorithms all estimate falling snow utilizing the higher frequency channels (166, 183 on GMI and Ka on DPR) to sense the characteristics of the frozen particles. These higher frequency channels were added to the design in 2006 after a series of papers showed that they were

useful for detecting and estimating falling snow (e.g., Kongoli et al., 2003; Chen and Staelin, 2003; Skofronick-Jackson et al.; 2004, Liu, 2004). Since launch, evaluations of GPM's falling snow retrieval performance are reported in Casella et al. (2017) and Tang et al. (2017).

Radiometer algorithms for uniform global precipitation estimates must be physically consistent across multiple frequencies and all constellation members. Bayesian or Optimal Estimation algorithms are well suited to retrieve precipitation and its vertical structure by comparing the information content of any multi-frequency radiometer to that supplied by a common *a priori* database of vertical profiles of precipitating clouds together with simulated Tb for each profile and sensor. By associating the combined algorithm's retrieved precipitation with DPR reflectivity profiles and GMI Tb, a robust global *a priori* database constrained by both DPR and GMI measurements is constructed, eliminating the need for *a priori* databases that rely solely on cloud resolving models. When the DPR does not detect precipitation but a precipitation signal is present in the 166 and 183 GHz channels of the GMI, CloudSat data is incorporated in the *a priori* database. This approach, designated as "radar-enhanced" radiometer algorithms, improves the accuracy and physical consistency among radiometer retrievals. While imagers and sounders typically have different channel sets and scanning procedures (conical versus cross-track), algorithm development is conceptually the same for all the passive sensors, with the Bayesian database reflecting the differences in instrumentation. Database Tb are computed from the geophysical parameters derived by the combined DPR/GMI retrievals so that differences in sensor channels, incidence angles and spatial resolutions are fully accounted for. Because of the variable surfaces features and impacts on precipitation, the Bayesian database is split into about 14 land surface classifications helping to improve the retrievals by minimizing the surface emissivity impacts. Since the same methodology can be used for previous as well as future sensors it is possible to extend GPM rainfall climatologies back to 1987 using SSM/I observations and potentially forward beyond the era of the GPM-CO satellite itself. A longer time series product will be released to the public in 2018.

While frequent coverage afforded by multiple constellation microwave radiometers is important, there

are as always, applications such as hydrology that require even greater temporal and spatial resolution. To this end, a number of multi-satellite techniques have been developed (see Ebert et al., 2007). One approach to ensuring uniform, frequent coverage is to use the passive microwave rainfall estimates as enhanced by geostationary-based IR observations such as IMERG and GSMaP (e.g., Kubota et al., 2007; 2017). GPM ensures that the microwave products being used for bias correction in these merged multi-satellite microwave/IR methods are consistent with one another. GPM also plans to explore ways to develop very-high spatial and temporal resolution (1-2 km and 5-10 minute) precipitation estimates through statistical downscaling or data assimilation using cloud-resolving models for certain hydrological applications.

In order to meet the objective (3) of the GPM mission, we also produce three-dimensional latent heating data. There are two representative latent heating algorithms, namely, Convective-Stratiform Heating (CSH) algorithm, which basically uses GMI data and utilizes convective/stratiform ratio with regionally produced latent heating tables, and Spectral Latent Heating (SLH) algorithm, which uses GPM DPR products with spectrally expressed tables for convective and stratiform precipitation separately. Latent heating data can be obtained as GPM standard products.

VII. Ground Validation

The NASA GPM program established a vigorous ground validation (GV) plan to use ground-based observations (including aircraft measurements) to support pre-launch satellite algorithm development and post-launch precipitation product evaluation. Three key components of the GPM GV infrastructure include numerous field campaigns and field site measurements, exploitation of NOAA's Multi-Radar Multi-Sensor (MRMS) products, and development of a Validation Network (VN) architecture described below. The field campaigns fully sampled precipitation at the surface, precipitation physics in the clouds, and conducted active/passive microwave remote sensing from above the clouds using ground, in situ and remote sensing aircraft, and satellite measurements. These field campaign data were instrumental both in developing the satellite retrieval algorithms by reducing the assumptions and in measuring integrated quantities for

hydrometeorological applications. MRMS data are rain gauge bias-adjusted radar estimates of precipitation rate and type (rain/snow) over the U.S. and neighboring territory (130°-60°W, 20°-55°N). GV MRMS datasets are derived from the NOAA MRMS products but are further processed (e.g., Kirstetter et al., 2012; 2015) to produce gauge-corrected reference precipitation rate datasets augmented with information on precipitation types and data quality at the native 2-minute/0.01° x 0.01° resolutions. The Validation Network (VN) radar data consists of ~80 U.S. network, oceanic, and/or other national/international research site-specific dual polarimetric (dual-pol) radars and their derived precipitation rate, DSD and hydrometeor type estimates that are footprint and geometrically volume-matched to GPM-CO overpasses (Bolen and Chandrasekar, 2003; Schwaller and Morris, 2011; Pippitt et al., 2015).

GPM GV precipitation measurement equipment inventory is vast (Skofronick-Jackson et al., 2017). Most equipment is designed to be portable for moving to field campaign locations as GPM continues to participate in precipitation related field campaigns worldwide. When not deployed for GPM-related field campaigns, these instruments operate within the NASA Wallops Flight Facility (WFF) network (or partner sites), with special emphasis placed on targeted and user-adapted data collections during GPM-CO overpasses to meet the needs and requests of the GPM algorithm and GV teams. All GV data is freely available from a link on the GPM webpage (gpm.nasa.gov).

VIII. Applications

Through improved measurements of rain and snow the GPM suite of products contributes to a wide range of societal applications such as: tropical and extratropical cyclone location and rainfall monitoring, famine early warning, drought monitoring, water resource management, agricultural forecasting, numerical weather prediction, land surface modeling, global climate modeling, disease tracking, economic studies, and animal migration; many of which were initially developed with TRMM data. Several of these applications require NRT data as well as longer-term, well-calibrated merged-satellite precipitation information (Reed et al., 2015); the GPM mission supports both of these product latencies. IMERG is being used as an input for forecasts (e.g., floods, landslides, agriculture/famine, precipitation-induced disease

outbreaks) in other regions of the world, especially areas lacking adequate ground-based information (Kidd et al., 2017). Selected applications are reported in Kirschbaum et al., (2017) and Kucera et al., (2013). GPM's remotely-sensed precipitation data enable a diverse range of applications across agencies, research institutions and the global community.

IX. SUMMARY

GPM is an international satellite mission to unify and advance precipitation measurements from a constellation of dedicated and operational microwave sensors to provide the next-generation unified global precipitation products for research and applications. GPM is a partnership between NASA and JAXA, with additional domestic and international partnerships. In February 2014, NASA and JAXA launched the GPM-CO in a 65°-inclined orbit carrying the first dual-frequency radar in space together with an advanced microwave radiometer serving as a precipitation physics observatory and calibration reference for all constellation radiometric measurements and retrievals.

GPM is a science mission with integrated applications goals to advance the knowledge of the global water/energy cycle variability and freshwater availability and improve weather, climate, and hydrological prediction capabilities. Within the framework of GEO and GEOSS, GPM serves as a cornerstone for the development of the CEOS Precipitation Constellation (PC). During its mission life, GPM is a mature realization of the CEOS-PC to provide state-of-the-art global precipitation products for scientific research and societal applications.

ACKNOWLEDGMENT

Contributions of the GPM Inter-Satellite Calibration Working Group, the Ground Validation Working Group, the GPM algorithm teams, and the PMM Science Team are gratefully acknowledged. Imagery assistance from the NASA Science Visualization Studio is greatly appreciated. Funding for these activities is provided by NASA Headquarters, primarily Ramesh Kakar.

REFERENCES

Berg W, Bilanow S, Chen R, Datta S, Draper D, Ebrahimi H, Farrar S, Jones WL, Kroodsma R, McKague D, Payne V, Wang J, Wilheit T, Yang JX (2016) Intercalibration of the GPM Radiometer Constellation. *J. Atmos. Oceanic Technol.* 33 : 2639 – 2654. DOI: 10.1175/JTECH-D-16-0100

Bolen S, Chandrasekar V. (2003) Methodology for aligning and comparing spaceborne radar and ground-based radar observations. *J. Atmos. Oceanic Technol*. 20 : 647 – 659. DOI: 10.1175/1520-0426(2003)20<647:MFAACS>2.0.CO;2

Brown, S. T. and C.S. Ruf (2005) Determination of a Hot Blackbody Reference Target over the Amazon Rainforest for the On-orbit Calibration of Microwave Radiometers, *AMS J. Oceanic Atmos. Tech*., 22(9), pp. 1340-1352

Casella, D., G. Panegrossi, P. Sanò, A. C. Marra, S. Dietrich, B. T. Johnson, and M. S. Kulie (2017) Evaluation of the GPM-DPR Snowfall Detection Capability: Comparison with CloudSat-CPR. *Atmos. Res*. doi: 10.1016/j.atmosres.2017.06.018

Chen, F. W. and D. H. Staelin (2003) AIRS/AMSU/HSB precipitation estimates, in IEEE Transactions on Geoscience and Remote Sensing, vol. 41, no. 2, pp. 410-417, doi: 10.1109/TGRS.2002.808322

Draper, DW, Newell DA, Wentz FJ, Krimchansky S, Skofronick-Jackson S. (2015a) The Global Precipitation Measurement (GPM) Microwave Imager (GMI): Instrument Overview and Early On-orbit Performance. *IEEE Journal of Selected Topics in Applied Earth Observations and Remote Sensing*. 8 : 3452 - 3462. DOI: 10.1109/JSTARS.2015.2403303

Draper, DW, Newell DA, McKague DS, Piepmeier JR (2015b) Assessing Calibration Stability Using the Global Precipitation Measurement (GPM) Microwave Imager (GMI) Noise Diodes. *IEEE Journal of Selected Topics in Applied Earth Observations and Remote Sensing*. 8 : 4239 - 4247. DOI: 10.1109/JSTARS.2015.2406661

Ebert, E., J. Janowiak, and C. Kidd (2007) Comparison of near real time precipitation estimates from satellite observations and numerical models," *Bull. Amer. Meteor. Soc.*, 88, pp. 47-64.

Goldberg, M. D., H. Kilcoyne, H. Cikanek, and A. Mehta (2013), Joint Polar Satellite System: The United States next generation civilian polar-orbiting environmental satellite system, J. Geophys. Res. Atmos., 118, 13,463–13,475, doi:10.1002/2013JD020389.

Gopalan, K., Jones, W.L., Biswas, S., Bilanow, S., Wilheit, T. and Kasparis, T., (2009) A time-varying radiometric bias correction for the TRMM microwave imager. IEEE Transactions on Geoscience and Remote Sensing, 47(11), pp.3722-3730.

Grecu, M., W. S. Olson, S. J. Munchak, S. Ringerud, L. Liao, Z. Haddad, B. L. Kelley, S. F. McLaughlin (2016) The GPM Combined Algorithm. J. Atmos. Oceanic Technol., 33, 2225-2245, doi:10.1175/JTECH-D-16-0019.1.

Hong, L., Jones, W.L., Wilheit, T.T. and Kasparis, T., (2009) Two approaches for inter-satellite radiometer calibrations between TMI and WindSat. Journal of the Meteorological Society of Japan. Ser. II, 87, pp.223-235.

Hou AY, Kakar RK, Neeck S, Azarbarzin AA, Kummerow CD, Kojima M, Oki R, Nakamura K, Iguchi T. (2014) The Global Precipitation Measurements Mission. *Bull. Amer. Meteor. Soc.* 95 : 701 - 722. DOI: 10.1175/BAMS-D-13-00164.1

Houze, R.A., L.A. McMurdie, W.A. Petersen, M.R. Schwaller, W. Baccus, J. Lundquist, C. Mass, B. Nijssen, S.A. Rutledge, D. Hudak, S. Tanelli, G.G. Mace, M. Poellot, D. Lettenmaier, J. Zagrodnik, A. Rowe, J. DeHart, L. Madaus, and H. Barnes, (2017) The Olympic Mountains Experiment (OLYMPEX). Bull. Amer. Meteor. Soc., 0, https://doi.org/10.1175/BAMS-D-16-0182.1

Huffman, G. J., R.F. Adler, D.T. Bolvin, G. Gu, E.J. Nelkin, K.P. Bowman, Y. Hong, E.F. Stocker, D.B. Wolff (2007) The TRMM Multi-satellite Precipitation Analysis: Quasi-Global, Multi-Year, Combined-Sensor Precipitation Estimates at Fine Scale. *J. Hydrometeor.*, 8(1), pp. 38-55.

Huffman GJ, Bolvin DT, Braithwaite D, Hsu K, Joyce R, Kidd C, Nelkin EJ, Sorooshian S, Tan J, Xie P. (2017) Algorithm Theoretical Basis Document (ATBD) Version 4.6 for the NASA Global Precipitation Measurement (GPM) Integrated Multi-satellitE Retrievals for GPM (I-MERG). 32pp. GPM Project: Greenbelt, MD. [Available online at https://pmm.nasa.gov/sites/default/files/document_files/IMERG_ATBD_V4.6.pdf]

Jensen, M.P., W.A. Petersen, A. Bansemer, N. Bharadwaj, L.D. Carey, D.J. Cecil, S.M. Collis, A.D. Del Genio, B. Dolan, J. Gerlach, S.E. Giangrande, A. Heymsfield, G. Heymsfield, P. Kollias, T.J. Lang, S.W. Nesbitt, A. Neumann, M. Poellot, S.A. Rutledge, M. Schwaller, A. Tokay, C.R. Williams, D.B. Wolff, S. Xie, and E.J. Zipser (2016) The Midlatitude Continental Convective Clouds Experiment (MC3E). Bull. Amer. Meteor. Soc., 97, 1667–1686, https://doi.org/10.1175/BAMS-D-14-00228.1

Kidd C, Huffman GJ, Becker A, Skofronick-Jackson G, Kirschbaum D, Joe P, Muller C (2017) So, how much of the Earth's surface *is* covered by rain gauges? *Bull. Amer. Meteor. Soc.* 98 : 69 - 78. DOI: 10.1175/BAMS-D-14-00283.1

Kidd, C., Tan, J., Kirstetter, P. and Petersen, W.A. (accepted 2017): Validation of the Version 05 Level 2 precipitation products from the GPM Core Observatory and constellation satellite sensors. *Accepted by Quarterly Journal of the Royal Meteorological Society*

Kirschbaum, DB, Huffman GJ, Adler RF, Braun S, Garrett K, Jones E, McNally A, Skofronick-Jackson G,

Stocker E, Wu H, Zaitchik BF (2017) NASA's Remotely-sensed Precipitation: A Reservoir for Applications Users. *Bull. Am. Meteorol. Soc.* 98 : 1169 – 1184. DOI: 10.1175/BAMS-D-15-00296.1

Kirstetter, P., Y. Hong, J. J. Gourley, S. Chen, Z. L. Flamig, J. Zhang, M. Schwaller, W. Petersen, E. Amitai (2012) Toward a framework for systematic error modeling of spaceborne precipitation radar with NOAA/NSSL ground radar-based National Mosaic QPE. *J. Hydrometeor.*, **13**, 1285-1300, doi:10.1175/JHM-D-11-0139.1

Kirstetter PE, Hong Y, Gourley JJ, Schwaller M, Petersen W, Cao Q (2015) Impact of sub-pixel rainfall variability on spaceborne precipitation estimation: evaluating the TRMM 2A25 product. *Q. Journal of the Royal Met. Soc.* 141 : 953 – 966. DOI: 10.1002/qj.2416

Klaes, K.D., M. Cohen, Y. Buhler, P. Schlüssel, R. Munro, A. Engeln, E. Clérigh, H. Bonekamp, J. Ackermann, J. Schmetz, and J. Luntama, (2007) An Introduction to the EUMETSAT Polar system. Bull. Amer. Meteor. Soc., 88, 1085–1096, https://doi.org/10.1175/BAMS-88-7-1085

Kongoli, C., P. Pellegrino, R. R. Ferraro, N. C. Grody, and H. Meng (2003), A new snowfall detection algorithm over land using measurements from the Advanced Microwave Sounding Unit (AMSU), Geophys. Res. Lett., 30, 1756, doi:10.1029/2003GL017177, 14.

Kubota, T., S. Shige, H. Hashizume, K. Aonashi, N. Takahashi, S. Seto, M. Hirose, Y. N. Takayabu, K. Nakagawa, K. Iwanami, T. Ushio, M. Kachi, and K. Okamoto (2007) Global Precipitation Map using Satelliteborne Microwave Radiometers by the GSMaP Project: Production and Validation, *IEEE Trans. Geosci. Rem. Sens.* 45, pp. 2259-2275.

Kubota, T., K. Aonashi, T. Ushio, S. Shige, Y. N. Takayabu, Y. Arai, T. Tashima, M. Kachi, Riko Oki, (2017) Recent Progress in Global Satellite Mapping of Precipitation (GSMaP) Product, Proc. IGARSS2017, Fort Worth, US.

Kucera PA, Ebert EE, Turk FJ, Levizzani V, Kirschbaum D, Tapiador FJ, Loew A, Borsche M. (2013) Precipitation from space: Advancing Earth system science. *Bull. Amer. Meteor. Soc.* 94 : 365 – 375. DOI: 10.1175/BAMS-D-11-00171.1

Kuo, K., W.S. Olson, B.T. Johnson, M. Grecu, L. Tian, T.L. Clune, B.H. van Aartsen, A.J. Heymsfield, L. Liao, and R. Meneghini, (2016) The Microwave Radiative Properties of Falling Snow Derived from Nonspherical Ice Particle Models. Part I: An Extensive Database of Simulated Pristine Crystals and Aggregate Particles, and Their Scattering Properties. J. Appl. Meteor. Climatol., 55, 691–708, https://doi.org/10.1175/JAMC-D-15-0130.1

Kummerow, C., J. Simpson, O. Thiele, W. Barnes, A.T.C. Chang, E. Stocker, R. F. Adler, A. Hou, R. Kakar, F. Wentz, P. Ashcroft, T. Kozu, Y. Hong, K. Okamoto, T. Iguchi, K Kuriowa, E. Im, Z. Haddad, G. Huffman, B. Ferrier, W. S. Olson, E. Zipser, E. A. Smith, T. T. Wilheit, G. North, T. Krishnamurti,

and K Nakamura (2000) The status of the Tropical Rainfall Measuring Mission (TRMM) after two years in orbit, *J. Appl. Meteor*., Vol. 39, No. 12, Part 1, pp. 1965-1982.

Kummerow, C., W. Barnes, T. Kozu, J. Shiue, and J. Simpson (1998) The Tropical Rainfall Measuring Mission (TRMM) Sensor Package, *J. Atmos. Oceanic Technol.*, Vol 15, pp. 809–817.

Kummerow CD, Randel DL, Kulie M, Wang NY, Ferraro R, Munchak SJ, Petkovic V. (2015) The Evolution of the Goddard Profiling Algorithm to a Fully Parametric Scheme. *J. Atmos. Oceanic Technol.* 32 : 2265 -2280. DOI: 10.1175/JTECH-D-15-0039.1

Kunkee, D. B. , G. Poe, D. Boucher, S. Swadley, Y. Hong, J. Wessl, and E. Uliana, (2008) Design and evaluation of the first Special Sensor Microwave Imager/Sounder, *IEEE Trans. Geosci. Rem. Sens*., Vol. 46, pp. 863-883.

Liao, L., and R. Meneghini (2005) A Study of Air/Space-borne Dual-Wavelength Radar for Estimation of Rain Profiles, *Advances in Atmospheric Sciences*, Vol. 22. No. 6, pp. 841-851.

Lin, X., and A. Y. Hou (2008) Evaluation of coincident passive microwave rainfall estimates using TRMM PR and ground-based measurements as references, *J. Appl. Meteoro. Climate*, Vol. 47, pp. 3170-3187.

Liu, G., (2004) Approximation of Single Scattering Properties of Ice and Snow Particles for High Microwave Frequencies. J. Atmos. Sci., 61, 2441–2456, https://doi.org/10.1175/1520-0469(2004)061<2441:AOSSPO>2.0.CO;2

Maeda, T., Y. Taniguchi and K. Imaoka, (2016) GCOM-W1 AMSR2 Level 1R Product: Dataset of Brightness Temperature Modified Using the Antenna Pattern Matching Technique, in IEEE Transactions on Geoscience and Remote Sensing, vol. 54, no. 2, pp. 770-782, doi: 10.1109/TGRS.2015.2465170

Meneghini, R., T. Iguchi, T. Kozu, L. Liao, K. Okamoto, J.A. Jones, and J. Kwiatkowski, (2000) Use of the Surface Reference Technique for Path Attenuation Estimates from the TRMM Precipitation Radar, *J. Appl. Meteor.*, 39, pp. 2053–2070, 2000.

Mugnai, A., et al., (2007) Snowfall measurements by the proposed European GPM Mission. In *Measuring Precipitation from Space: EURAINSAT and the future*. Eds. V. Levizzani, P. Bauer and J. Turk. Springer-Verlag, 750 pp.

Nayak, M.A., G. Villarini, and A.A. Bradle (2016) Atmospheric Rivers and Rainfall during NASA's Iowa Flood Studies (IFloodS) Campaign. J. Hydrometeor., 17, 257–271, https://doi.org/10.1175/JHM-D-14-0185.1

Olson, W. S., L. Tian, M. Grecu, K.-S. Kuo, B. T. Johnson, A. J. Heymsfield, A. Bansemer, G. M. Heymsfield, J. R. Wang, and R. Meneghini (2017) The Microwave Radiative Properties of Falling Snow Derived from Nonspherical Ice Particle Models. Part II: Initial Testing Using Radar, Radiometer

and In Situ Observations. J. Appl. Meteor. Climatol., 55, 709-722, doi:10.1175/JAMC-D-15-0131.1.

Pippitt J, Wolff DB, Petersen WA, Marks D. (2015) Data and operational processing for NASA's GPM ground validation program. *37th Conf. on Radar Meteorology, Norman, OK 16 Sept 2015.* American Meteorological Society: Boston.

Reed PM, Chaney NW, Herman JD, Ferringer MP, Wood EF. (2015) Internationally coordinated multi-mission planning is now critical to sustain the space-based rainfall observations needed for managing floods globally. *Environ. Res. Lett.* 10 : 024010. DOI: 10.1088/1748-9326/10/2/024010

Rémy, R., Brogniez Hélène, Chambon Philippe, Chomette Olivier, Cloché Sophie, Gosset Marielle E., Mahfouf Jean-Francois, Raberanto Patrick, Viltard Nicolas, (2015) The Megha-Tropiques mission: a review after three years in orbit, Frontiers in Earth Science, vol. 3, DOI=10.3389/feart.2015.00017

Ruf, C. S., Y. Hu and S.T. Brown, (2006) Calibration of WindSat Polarimetric Channels with a Vicarious Cold Reference, *IEEE Trans. Geosci. Remote Sens*., 44(3), pp. 470-475.

Schwaller, M. R., and K. R. Morris, (2011) A Ground Validation Network for the Global Precipitation Measurement Mission. *J. Atmos. Oceanic Technol*., **28**, 301–319, doi:10.1175/2010JTECHA1403.1.

Skofronick-Jackson, G., D. Hudak, W. Petersen, S.W. Nesbitt, V. Chandrasekar, S. Durden, K.J. Gleicher, G. Huang, P. Joe, P. Kollias, K.A. Reed, M.R. Schwaller, R. Stewart, S. Tanelli, A. Tokay, J.R. Wang, and M. Wolde, (2015) Global Precipitation Measurement Cold Season Precipitation Experiment (GCPEX): For Measurement's Sake, Let It Snow. Bull. Amer. Meteor. Soc., 96, 1719–1741, https://doi.org/10.1175/BAMS-D-13-00262.1

Skofronick-Jackson, G.M., Kim, M.J., Weinman, J.A. and Chang, D.E., (2004) A physical model to determine snowfall over land by microwave radiometry. IEEE Transactions on Geoscience and Remote Sensing, 42(5), pp.1047-1058.

Skofronick-Jackson, G., W. A. Petersen, W. Berg, C. Kidd, E. F. Stocker, D. B. Kirschbaum, R. Kakar, S. A. Braun, G. J. Huffman, T. Iguchi, P. E. Kirstetter, C. Kummerow, R. Meneghini, R. Oki, W. S. Olson, Y. N. Takayabu, K. Furukawa, and T. Wilheit, (2017) The Global Precipitation Measurement (GPM) Mission for Science and Society. Bull. Amer. Meteor. Soc., doi:10.1175/BAMS-D-15-00306.1.

Stephens, G. L., and C. D. Kummerow, (2007) The remote sensing of clouds and precipitation from space: A review, *J. Atmos. Science*, Vol. 64, pp. 3742-3765.

Tang, G., Y. Wen, J. Gao, D. Long, Y. Ma, W. Wan, and Y. Hong (2017) Similarities and differences between three coexisting spaceborne radars in global rainfall and snowfall estimation, *Water Resour. Res*., 53, doi:10.1002/2016WR019961.

Wentz, F. and D. Draper, (2016) On-orbit absolute calibration of the Global Precipitation Mission Microwave Imager, *J. Atmos. Oceanic Tech*., **33**, 1393-1412, doi: 10.1175/JTECH-D-15-0212.1.

Zhang J, Howard K, Langston C, Kaney B, Qi Y, Tang L, Grams H, Wang Y, Cocks S, Martinaitis S, Arthur A, Cooper K, Brogden J. (2016) Multi-Radar Multi-Sensor (MRMS) Quantitative Precipitation Estimation: Initial Operating Capabilities. *Bull. Amer. Meteor. Soc.* 97 : 621 – 638. DOI: 10.1175/BAMS-D-14-00174.1

Figure Captions:

Figure 1: GMI and DPR precipitation retrievals from the GPM Core Observatory observing a March 17, 2014 snow storm..

Figure 2: The GPM constellation in 2017 includes the GPM Core Observatory and constellation radiometers on partner satellites (Megha-Tropiques, GCOM-W1, DMSP F18 and F19, NPP, NOAA-19, MetOp-B, and NPOESS C1).

Table Captions:

Table 1: GPM-CO GMI and DPR specifications and on-orbit performance.

Table 2: GPM-CO and constellation partner passive microwave radiometer sensor capabilities in 2017.

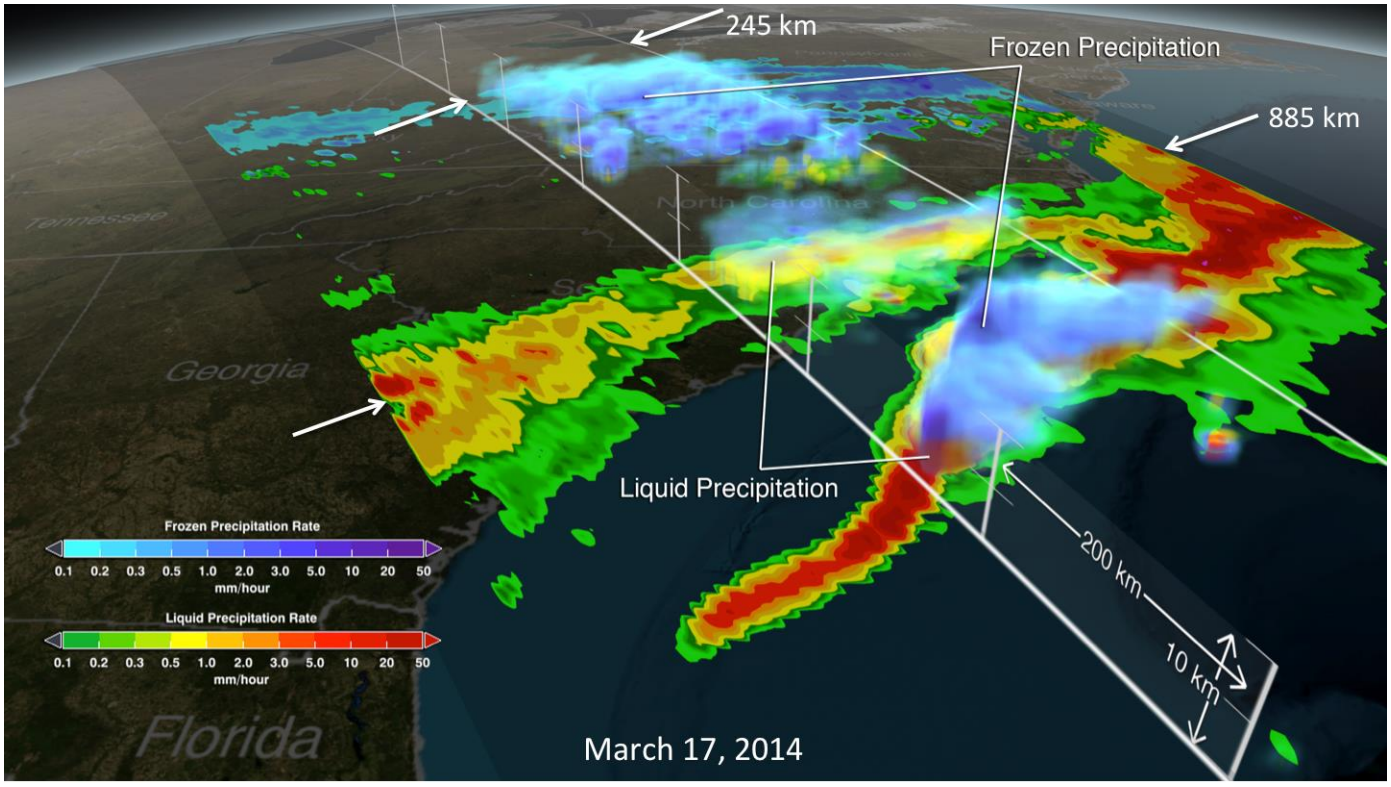

Figure 1: GMI and DPR precipitation retrievals from the GPM Core Observatory observing a March 17, 2014 snow storm.

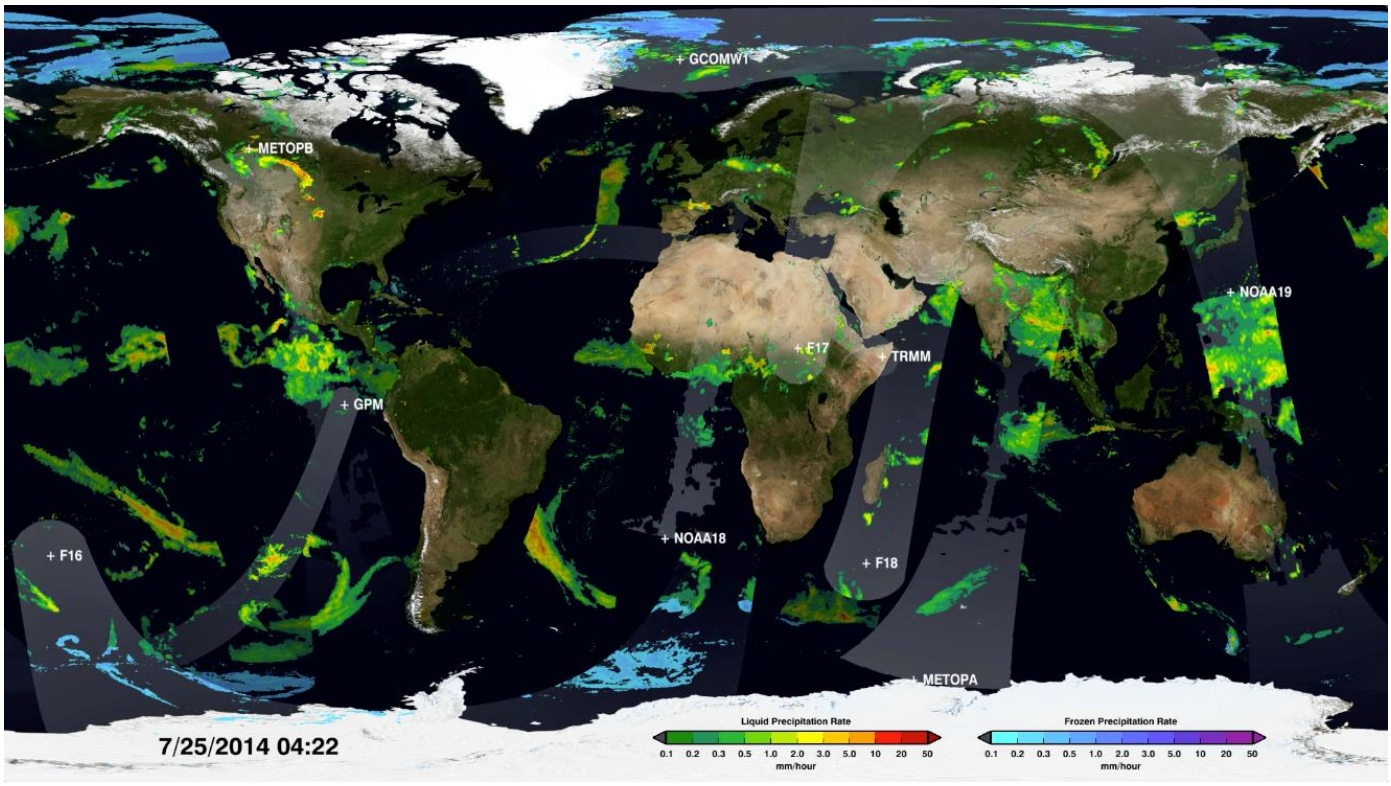

Figure 2: The GPM constellation in 2017 includes the GPM Core Observatory and constellation radiometers on partner satellites (Megha-Tropiques, GCOM-W1, DMSP F18 and F19, NPP, NOAA-19, MetOp-B, and NPOESS C1).

Table 1: GPM-CO GMI and DPR specifications and on-orbit performance.

Channel (GHz)	Spatial Resolution (km)	NEDT (K) (required)	NEDT (K) (on orbit)	Beamwidth in degrees (on orbit)	Beam Efficiency in % (on orbit)
GMI 10.65 V-pol	19.4 x 32.1	0.96	0.77	1.72	91
GMI 10.65 H-pol	19.4 x 32.1	0.96	0.78	1.72	91
GMI 18.7 V-pol	10.9 x 18.1	0.84	0.63	0.98	91
GMI 18.7 H-pol	10.9 x 18.1	0.84	0.60	0.98	91
GMI 23.8 V-pol	9.7 x 16.0	1.05	0.51	0.85	93
GMI 36.64 V-pol	9.4 x 15.6	0.65	0.41	0.82	98
GMI 36.64 H-pol	9.4 x 15.6	0.65	0.42	0.82	98
GMI 89 V-pol	4.4 x 7.2	0.57	0.32	0.38	97
GMI 89 H-pol	4.4 x 7.2	0.57	0.31	0.38	97
GMI 166 V-pol	4.1 x 6.3	1.5	0.70	0.38	97
GMI 166 H-pol	4.1 x 6.3	1.5	0.66	0.37	97
GMI 183.31±3 V-pol	3.8 x 5.8	1.5	0.56	0.37	95
GMI 183.31±7 V-pol	3.8 x 5.8	1.5	0.47	0.37	95
DPR 13.6 (Ku)	5 km horizontally 250 m vertically (oversampled to 125 km)	Minimum detectable reflectivity ~12-13 dBZ			
DPR 35.5 (Ka)	5 km horizontally 250 m vertically 500 m vertically in	Minimum detectable reflectivity ~17-18 dBZ (~12-13 dBZ in high sensitivity mode)			

	high sensitivity mode (oversampled to 125 km and 250 km, respectively)	

Table 2. GPM-CO and constellation partner passive microwave radiometer sensor capabilities in 2017.

Channel[1]	6-7 GHz	10 GHz	19 GHz	23 GHz	31-37 GHz	50-60 GHz	89-91 GHz	150-167 GHz	183-190 GHz
GMI		10.65 V/H	18.70 V/H	23.80 V	36.50 V/H		89.0 V/H	165.6 V/H	183.31±3 V 183.31±8 V
Resolution[2]		26km	15km	12km	11km		6km	5km	5km
AMSR 2	6.925/7.3 V/H	10.65 V/H	18.70 V/H	23.80 V/H	36.5 V/H		89.0 V/H		
Resolution[2]	62/58km	42km	22km	26km	12km		5km		
SSMIS			19.35 V/H	22.235 V	37.0 V/H	50.3-63.28 V/H	91.65 V/H	150 H	183.31±1 H 183.31±3 H 183.31±7 H
Resolution[2]			59km	59km	36km	22km	14km	14km	14km
SAHPIR									183.31±0.2 QH 183.31±1.1 QH 183.31±2.8 QH 183.31±4.2 QH 183.31±6.8 QH 183.31±11 QH
Resolution[2]									10km
MHS							89 QV	157 QV	183.31±1 QH 183.31±3 QH
Resolution[2]							17km	17km	190.311 QV

									17km
ATMS				23.8 QV	31.4 QV	50.3-57.29 QH	87-91 QV	165.5 H QH	183.31±1 QH 183.31±1.8 QH 183.31±3 QH 183.31±4.5 QH 183.31±7 QH
Resolution[2]				74km	74km	32km	16km	16km	16km

[1]Channel Center Frequency (GHz): V–Vertical Polarization, H-Horizontal Polarization, QV-Quasi-Vertical, QH-Quasi-Horizontal (QV and QH indicates mixed polarization for cross-track scanners).

[2]Mean spatial resolution (km)